


Cite this: *RSC Adv.*, 2020, 10, 39617

# <sup>17</sup>O NMR spectroscopy-assisted *in vitro* bioactivity studies of the intermediates formed *via* Na<sub>2</sub>S and RSNO cross-linking reactions

Xingyu Zhu and Yin Gao \*

The cross-linking reaction between sulfide and *S*-nitrosothiol moieties has been intensively investigated and thionitrite/thionitrous acid (SNO<sup>−</sup>/HSNO) as well as nitrosopersulfide (SSNO<sup>−</sup>) were reported to be the intermediates that could serve as reservoirs for nitric oxide (NO). However, debate still exists regarding the stability and biological activity of SNO<sup>−</sup>/HSNO and SSNO<sup>−</sup>. In order to investigate the chemical properties and biological activity of SNO<sup>−</sup> and SSNO<sup>−</sup>, we set out to re-characterize the reaction intermediates using UV-Vis and <sup>15</sup>N NMR spectroscopy techniques, as well as a new <sup>17</sup>O NMR approach. The effects of SNO<sup>−</sup> and SSNO<sup>−</sup> on cellular NO and cGMP levels were assessed *via* cell culture experiments, and also the effects of SNO<sup>−</sup> and SSNO<sup>−</sup> on cell proliferation, migration, and capillary-like structure formation were evaluated with human umbilical vein endothelial cells (HUVEC). Through this work, the characteristic peaks and half-lives of SNO<sup>−</sup> and SSNO<sup>−</sup> were elucidated under various preparation conditions. The biological assays demonstrated that SSNO<sup>−</sup> increased the cellular NO and cGMP levels and also facilitated cell proliferation, migration and stimulated angiogenesis, while in contrast SNO<sup>−</sup> did not exhibit these effects.

Received 8th June 2020  
Accepted 22nd October 2020

DOI: 10.1039/d0ra05054g

rsc.li/rsc-advances

## Introduction

Although hydrogen sulfide (H<sub>2</sub>S) is widely known as a noxious gas, it has also emerged as an important intracellular signal transducer along with nitric oxide (NO) and carbon monoxide (CO), which are involved in many physiological processes.<sup>1</sup> H<sub>2</sub>S exhibits similar biological effects to those of NO in terms of vascular tone regulation and control of blood pressure.<sup>2</sup> Both H<sub>2</sub>S and NO are endogenously synthesized in biological systems through precise enzymatic mechanisms.<sup>3</sup> These two gases usually exert similar and partially interdependent biological effects, which can lead to different chemical and biological reactions that attenuate or enhance each other.<sup>4</sup> For example, H<sub>2</sub>S acts as an enhancer of NO to promote vasodilation, but can also reverse the effects of NO to induce vasoconstriction.<sup>5,6</sup> The cross-linking reaction between H<sub>2</sub>S and NO has been well established. Recent studies have shown that polysulfide or thiol species formed from the reaction between H<sub>2</sub>S and NO were possible H<sub>2</sub>S-derived signaling molecules.<sup>7,8</sup> The interaction of H<sub>2</sub>S with NO or NO donors can activate neuroendocrine signaling pathways to regulate vasodilation and control meningeal blood flow.<sup>9,10</sup>

The reaction between sulfide and *S*-nitrosothiols has been extensively investigated, and thionitrite/thionitrous acid (SNO<sup>−</sup>/

HSNO) as well as nitrosopersulfide (SSNO<sup>−</sup>) have been reported to be the intermediates that serve as reservoirs for NO.<sup>11</sup> However, the stability and bioactivity of SNO<sup>−</sup>/HSNO and SSNO<sup>−</sup> have been subjects of lively debate<sup>11–14</sup> since the characterization of HSNO by electrospray ionization time-of-flight mass spectrometry (ESI-TOF-MS) and <sup>15</sup>N NMR spectroscopy under physiological conditions was first reported in 2012.<sup>15</sup> In the studies by Filipovic and coworkers, the smallest reported *S*-nitrosothiol HSNO was prepared *via* the reaction between *S*-nitrosoglutathione GSNO/GS<sup>15</sup>NO and Na<sub>2</sub>S (at a 1 : 1 molar ratio) in phosphate buffer at pH = 7.4. The *m/z* peak of 64 Da that was obtained *via* positive mode ESI-TOF-MS analysis was attributed to the [HSNO + H<sup>+</sup>] species. Meanwhile, the <sup>15</sup>N NMR spectrum showed a peak at 322 ppm which was reported to be the chemical shift of HSNO/SNO<sup>−</sup>.<sup>15</sup> However, Cortese-Krott and coworkers were unable to reproduce the aforementioned MS data nor the <sup>15</sup>N NMR spectrum in their lab.<sup>12</sup> They found that SNO<sup>−</sup> was very unstable and was immediately replaced by a more stable species, SSNO<sup>−</sup>, which they had reported to actually account for the sustained bioactivity of NO.<sup>16–19</sup> However, Filipovic and coworkers stated that the SSNO<sup>−</sup> species was a rather unstable intermediate that was sensitive to light, water and acid, which also could further react with H<sub>2</sub>S to generate HSNO. They claimed that the HSNO species rather than SSNO<sup>−</sup>, was the one that would actually induce cell signaling events.<sup>13,20</sup>

Up to now the chemical properties and bioactivity of SNO<sup>−</sup> and SSNO<sup>−</sup> still have not been fully elucidated. Although the

Key Laboratory for Molecular Enzymology and Engineering of Ministry of Education, School of Life Sciences, Jilin University, Changchun 130012, China. E-mail: yin.gao@queensu.ca



absorption spectroscopy of the sulfide and *S*-nitrosothiols cross-linking reaction intermediates has been intensively studied, these studies are still under debate due to the lack of chemical evidence, and opposing opinions have been raised regarding the absorbance peaks of  $\text{SNO}^-$  and  $\text{SSNO}^-$ .<sup>13,17–19,21,22</sup> In the current study, we endeavored to re-characterize the  $\text{SNO}^-$  and  $\text{SSNO}^-$  intermediates using UV-Vis and  $^{15}\text{N}$  NMR spectroscopy techniques as well as a new  $^{17}\text{O}$  NMR approach. In addition, the bioactivity of  $\text{SNO}^-$  and  $\text{SSNO}^-$  was assessed by using cultured human umbilical vein endothelial cells (HUVEC).

## Results and discussion

Fig. 1 shows the UV-Vis spectroscopy spectra of the intermediates that were formed by cross-linking reactions between *S*-nitroso-*N*-acetylpenicillamine SNAP and  $\text{Na}_2\text{S}$  under aqueous and non-aqueous conditions. As shown in Fig. 1a, immediately after SNAP and  $\text{Na}_2\text{S}$  (at a 1 : 1 ratio) had been mixed in DMSO, the absorption at 340 nm was the only peak that was observed in the initial spectrum (red line). As time progressed, the absorbance of the peak at 340 nm diminished while that of a new peak at 450 nm gradually increased. We assumed that these two peaks respectively represented the intermediates  $\text{SNO}^-$  and

$\text{SSNO}^-$ , which had formed *via* the cross-linking reaction based on earlier studies by other researchers.<sup>17</sup> To support our hypothesis, we have previously proposed a reaction pathway for the generation of  $[\text{Fe}(\text{CN})_5\text{N}(\text{O})\text{S}]^{4-}$  and  $[\text{Fe}(\text{CN})_5\text{N}(\text{O})\text{SS}]^{4-}$  during the Gmelin reaction, in which  $[\text{Fe}(\text{CN})_5\text{N}(\text{O})\text{S}]^{4-}$  was the first intermediate formed after the mixing of sodium nitroprusside ( $[\text{Fe}(\text{CN})_5\text{NO}]^{2-}$ ) and  $\text{Na}_2\text{S}$ .<sup>23</sup>  $[\text{Fe}(\text{CN})_5\text{N}(\text{O})\text{S}]^{4-}$  subsequently decomposed relatively quickly (with a half-life of 1.5 min), and was replaced by  $[\text{Fe}(\text{CN})_5\text{N}(\text{O})\text{SS}]^{4-}$  as a relatively stable intermediate.<sup>23</sup> For this reason, we proposed that the absorption signal at 340 nm represented  $\text{SNO}^-$ , while  $\text{SSNO}^-$  exhibited an absorption band at 450 nm.

Based on this assumption, in the cases in which equimolar amounts of SNAP and  $\text{Na}_2\text{S}$  were mixed in DMSO, all of the SNAP would have been converted to  $\text{SNO}^-$  initially, and would subsequently react with  $\text{HSS}^-$  to form  $\text{SSNO}^-$ . However, once the SNAP :  $\text{Na}_2\text{S}$  molar ratio was changed to 1 : 0.5, peaks at both 340 and 450 nm were observed immediately after mixing, and grew weaker as time progressed. This could be due to the excess of SNAP that might have reacted with both  $\text{HS}^-$  and  $\text{HSS}^-$  to generate  $\text{SNO}^-$  and  $\text{SSNO}^-$  simultaneously, or at least the two peaks were visible at the same time (Fig. 1b). In comparison, the reaction that was performed in DMF exhibited similar spectra with those recorded in DMSO, as shown in Fig. 1c and d. In contrast, when SNAP and  $\text{Na}_2\text{S}$  were mixed in phosphate buffer at pH 7.4, the absorption peak representing  $\text{SNO}^-$  shifted from 340 to 329 nm, while that corresponding to  $\text{SSNO}^-$  had shifted from 450 to 412 nm (Fig. 1e). Additionally, a higher molar equivalent of  $\text{Na}_2\text{S}$  was required to convert all of the SNAP to  $\text{SNO}^-$  than was needed for the corresponding reactions performed in DMSO and DMF, since  $\text{HS}^-$  behaves as a stronger nucleophile in a non-aqueous solvent than in aqueous environments.<sup>11,24</sup> Therefore, the spectra observed during the formation of  $\text{SNO}^-$  and  $\text{SSNO}^-$  *via* the mixing of equimolar amounts of SNAP and  $\text{Na}_2\text{S}$  in phosphate buffer were similar to those recorded during the formation of  $\text{SNO}^-$  and  $\text{SSNO}^-$  (1 : 0.5 molar ratio, SNAP :  $\text{Na}_2\text{S}$ ) in non-aqueous solvents (Fig. 1b and d).

When 2 molar equivalents of  $\text{Na}_2\text{S}$  were mixed with one equivalent of SNAP in phosphate buffer, a weak absorption at 329 nm ( $\text{SNO}^-$ ) and a strong absorption at 412 nm ( $\text{SSNO}^-$ ) were observed in the first recorded spectrum (Fig. 1f).  $\text{SNO}^-$  was then quickly replaced by  $\text{SSNO}^-$ , thus causing the peak at 412 nm to grow in the second minute (blue line). However,  $\text{SSNO}^-$  also eventually decomposed, suggesting that both  $\text{SNO}^-$  and  $\text{SSNO}^-$  were less stable in aqueous media than in non-aqueous solvents.

Although UV-vis spectroscopy is a convenient and relatively fast characterization method, it only provides relatively little structural application cannot be used alone to directly confirm the formation of a particular species. Meanwhile,  $^{15}\text{N}$  nuclei usually have very long spin-lattice relaxation times, so that a long acquisition time is required to obtain a  $^{15}\text{N}$  NMR spectrum. However, UV-Vis analysis showed that one of the intermediates was very unstable and only lasted briefly in phosphate buffer, which would limit the usefulness of  $^{15}\text{N}$  NMR spectroscopy for the detection of this intermediate. With these

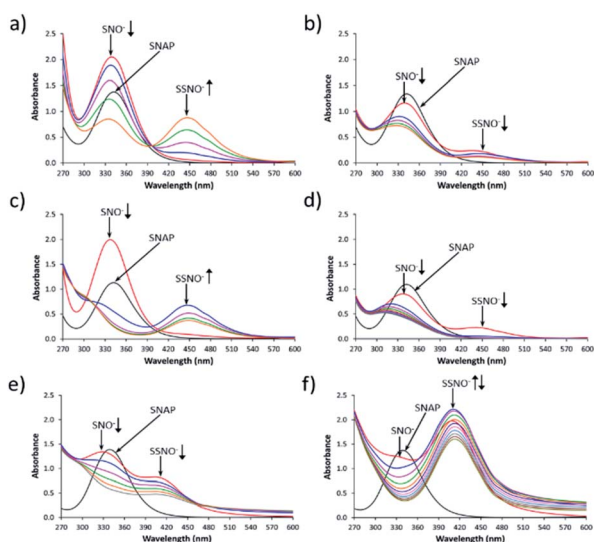
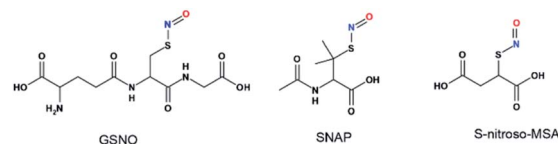


**Fig. 1** Reaction of SNAP and  $\text{Na}_2\text{S}$ . UV-Vis spectra were recorded every min after the mixing of SNAP with  $\text{Na}_2\text{S}$ . The line in black was SNAP, the line in red was the first spectrum that was recorded immediately after mixing (0 min), which was followed in sequence at 1 min intervals by the lines in blue (1 min), pink (2 min), green (3 min), and orange (4 min). (a) Mixing of 1.5 mM SNAP and 1 molar equivalent of  $\text{Na}_2\text{S}$  in DMSO. The signal at  $\lambda_{\text{max}} = 340$  nm can be attributed to  $\text{SNO}^-$ , while that at  $\lambda_{\text{max}} = 450$  nm corresponds to  $\text{SSNO}^-$ . (b) Reaction of 1.5 mM SNAP and 0.5 molar equivalents (0.75 mM) of  $\text{Na}_2\text{S}$  in DMSO. (c) Reaction of 1.5 mM SNAP and 1 molar equivalent of  $\text{Na}_2\text{S}$  in DMF. (d) Reaction of 1.5 mM SNAP and 0.5 molar equivalents of  $\text{Na}_2\text{S}$  in DMF. (e) Reaction of 1.5 mM SNAP and 1 molar equivalent of  $\text{Na}_2\text{S}$  in 0.5 M phosphate buffer at pH 7.4. The signal at  $\lambda_{\text{max}} = 329$  nm represents  $\text{SNO}^-$ , while that at  $\lambda_{\text{max}} = 412$  nm is attributed to  $\text{SSNO}^-$ . The intensity of the  $\text{SSNO}^-$  band increased during the first 2 min and subsequently diminished. (f) Reaction of 1.5 mM SNAP and 2 molar equivalents  $\text{Na}_2\text{S}$  in 0.5 M phosphate buffer at pH 7.4.



considerations in mind, we decided to explore the utility of  $^{17}\text{O}$  ( $I = 5/2$ ) NMR spectroscopy, which offers short acquisition times due to the rapid relaxation of this nucleus. As  $^{17}\text{O}$  has a very low natural abundance (0.037%), we first prepared  $^{17}\text{O}$ -labeled SNAP and GSNO and then allowed these species to react with  $\text{Na}_2\text{S}$  to generate  $^{17}\text{O}$ -labeled  $\text{SNO}^-$  and  $\text{SSNO}^-$ . GSNO is water soluble, and  $^{17}\text{O}$ -labeled GSNO exhibited a rather broad  $^{17}\text{O}$  NMR signal at  $\delta = 1211.6$  ppm with a full-width at the half height (FWHH) of 3552 Hz (Fig. 2a). Meanwhile, the  $^{17}\text{O}$ -labeled SNAP exhibits a narrower  $^{17}\text{O}$  NMR signal at  $\delta = 1296.0$  ppm with a FWHH of 1560 kHz (Fig. 2b). These  $^{17}\text{O}$  chemical shifts are comparable to that exhibited by the *S*-nitrosothiols RSNO ( $R = -\text{CH}(\text{COO}^-)(\text{CH}_2-\text{COO}^-)$ ) that was prepared with 2-mercaptosuccinic acid (MSA) and  $\text{NaNO}_2$  at  $\delta = 1200$  ppm and  $[\text{Fe}(\text{CN})_5\text{N}(\text{O})\text{SR}]^{3-}$  ( $R = -\text{CH}(\text{COO}^-)(\text{CH}_2-\text{COO}^-)$ ) at  $\delta = 1035$  ppm (FWHH = 4600 kHz) (Scheme 1).<sup>25</sup> These broad  $^{17}\text{O}$  NMR signals are due to the relatively large size of the RSNO molecules, which induces a very rapid  $^{17}\text{O}$  nuclear quadrupole relaxation. Upon the addition of one molar equivalent of  $\text{Na}_2\text{S}$  to the GSNO in phosphate buffer, only one sharp  $^{17}\text{O}$  NMR signal was detected at  $\delta = 896.5$  ppm (FWHH = 513 Hz) (Fig. 2c). As seen in Fig. 1f,  $\text{SNO}^-$  decomposed faster than  $\text{SSNO}^-$ , and  $\text{SNO}^-$  had decomposed completely during the acquisition of the spectra. Therefore, this  $^{17}\text{O}$  NMR signal observed in Fig. 2c can be attributed to  $\text{SSNO}^-$ , which has better stability.

Since both of these intermediates were less stable in aqueous media, the reaction was also performed in DMF by mixing SNAP



**Scheme 1** Structures of *S*-nitrosothiols. GSNO : *S*-nitrosoglutathione, SNAP : *S*-nitroso-*N*-acetylpenicillamine, and *S*-nitroso-MSA : *S*-nitroso-mercaptosuccinic acid.

with  $\text{Na}_2\text{S}$  (at a 1 : 1 molar ratio). SNAP is relatively hydrophobic and poorly soluble in water, but is soluble in DMF. The signal of SNAP in DMF was detected at  $\delta = 1311.6$  ppm (FWHH = 1152 Hz) (Fig. 2d). After mixing SNAP with  $\text{Na}_2\text{S}$  (at a 1 : 1 molar ratio) in DMF only one sharp signal was observed at  $\delta = 987.1$  ppm (FWHH = 268 Hz) (Fig. 2e), NMR signals (Fig. 2d and e) were narrower in DMF and the chemical shifts had moved downfield, evidently due to the hydrophobicity of the solvent. After many attempts, we were still unable to obtain the  $^{17}\text{O}$  NMR signal of  $\text{SNO}^-$  in these reaction mixtures. Therefore, we used triphenylphosphine (TPH) to reduce  $\text{SSNO}^-$  to  $\text{SNO}^-$  with the product of triphenylphosphine sulfide (TPH-S). By adding excess of TPH to  $\text{SSNO}^-$ , a sharp signal was obtained at  $\delta = 1209.6$  ppm (FWHH = 176 Hz), which can be attributed to  $\text{SNO}^-$  (Fig. 2f). This finding was consistent with our previous  $^{17}\text{O}$  NMR data obtained for  $[\text{Fe}(\text{CN})_5\text{N}(\text{O})\text{S}]^{4-}$  and  $[\text{Fe}(\text{CN})_5\text{N}(\text{O})\text{SS}]^{4-}$  intermediates that were formed in the Gmelin reaction, in which  $[\text{Fe}(\text{CN})_5\text{N}(\text{O})\text{S}]^{4-}$  exhibited a  $^{17}\text{O}$  NMR signal at  $\delta =$

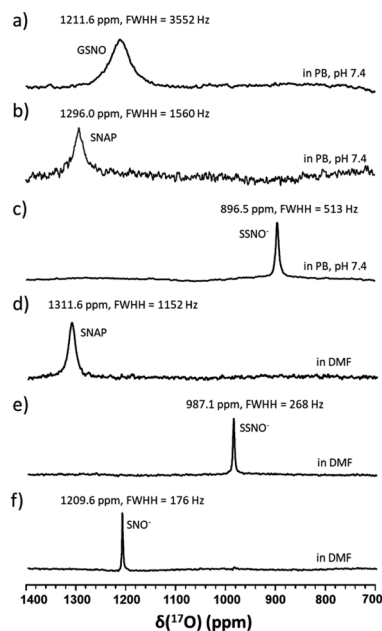


**Fig. 2**  $^{17}\text{O}$  NMR spectra of (a) 10 mM  $^{17}\text{O}$ -labeled GSNO in phosphate buffer pH 7.4, (b) 1.5 mM  $^{17}\text{O}$ -labeled SNAP in phosphate buffer pH 7.4, (c) freshly prepared  $^{17}\text{O}$ -labeled  $\text{SSNO}^-$  that was obtained by mixing 10 mM  $^{17}\text{O}$ -labeled GSNO with 1 molar equivalent of  $\text{Na}_2\text{S}$  in 1 M phosphate buffer at pH 7.4, (d) 100 mM  $^{17}\text{O}$ -labeled SNAP in DMF, (e) freshly prepared  $^{17}\text{O}$ -labeled  $\text{SSNO}^-$  that was obtained by mixing 100 mM  $^{17}\text{O}$ -labeled SNAP with 1 molar equivalent of  $\text{Na}_2\text{S}$  in DMF containing 10%  $\text{D}_2\text{O}$ , and (f) freshly prepared  $^{17}\text{O}$ -labeled  $\text{SNO}^-$  that was obtained by adding 6 molar equivalents of TPH to  $\text{SSNO}^-$ . TPH: triphenylphosphine.

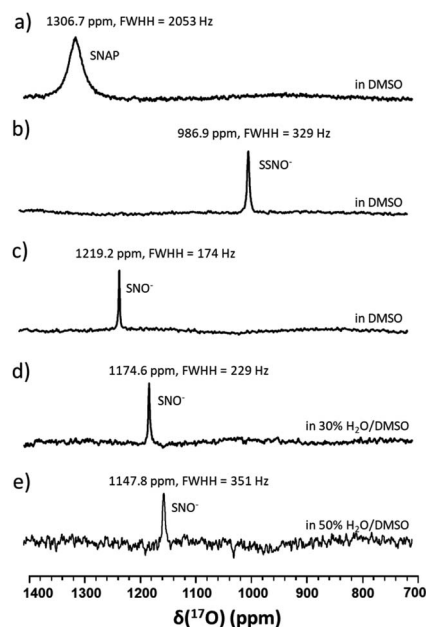


**Fig. 3**  $^{17}\text{O}$  NMR spectra of (a) 100 mM  $^{17}\text{O}$ -labeled SNAP in DMSO, (b) freshly prepared  $^{17}\text{O}$ -labeled  $\text{SSNO}^-$  that was obtained by mixing 100 mM  $^{17}\text{O}$ -labeled SNAP with 1 molar equivalent of  $\text{Na}_2\text{S}$  in DMSO containing 10%  $\text{D}_2\text{O}$ , (c) freshly prepared  $^{17}\text{O}$ -labeled  $\text{SNO}^-$  that was obtained by adding 2 molar equivalents of TPH to  $\text{SSNO}^-$ , (d) a spectrum recorded after water was added to  $\text{SNO}^-$  to yield 30%  $\text{H}_2\text{O}$  in DMSO, and (e) a spectrum recorded after water was added to  $\text{SNO}^-$  to yield 50%  $\text{H}_2\text{O}$  in DMSO.



1027 ppm and  $[\text{Fe}(\text{CN})_5\text{N}(\text{O})\text{SS}]^{4-}$  exhibited a  $^{17}\text{O}$  NMR signal at  $\delta = 938$  ppm.<sup>23</sup>

$^{17}\text{O}$ -Labelled  $\text{SSNO}^-$  and  $\text{SNO}^-$  were prepared in the same manner in DMSO, and similar chemical shifts were detected regardless of the solvent effect (Fig. 3a–c). However, upon the addition of  $\text{D}_2\text{O}$ , the NMR signals shifted to lower chemical shifts due to the electron shielding effect, which was due to the more hydrophilic surrounding environment (Fig. 3d and e). Filipovic and coworkers have recorded the  $^{15}\text{N}$  NMR signal of  $\text{HSNO}/\text{SNO}^-$  under conditions, but we found that  $\text{SNO}^-$  is very sensitive in the presence of water, and decomposed very rapidly.

In particular, it was difficult to detect the  $^{17}\text{O}$  NMR signal of  $\text{SNO}^-$  when the percentage of water exceeded 50% in DMSO. Since we also attempted to obtain the  $^{15}\text{N}$  NMR signals of the  $\text{SSNO}^-$  and  $\text{SNO}^-$  species in DMSO and in water–DMSO mixtures. Firstly,  $^{15}\text{N}$ -labeled SNAP was prepared and then allowed to react with  $\text{Na}_2\text{S}$  to generate  $\text{SNO}^-$  and  $\text{SSNO}^-$ . As seen in Fig. 4a,  $^{15}\text{N}$ -labeled SNAP exhibited a  $^{15}\text{N}$  NMR signal at  $\delta = 836.7$  ppm (relative to liquid  $\text{NH}_3$ ). This  $^{15}\text{N}$  chemical shift is comparable to that exhibited by the  $\text{RSNO}$  ( $\text{R} = -\text{CH}(\text{COO}^-)(\text{CH}_2)-\text{COO}^-$ ) at  $\delta = 761$  ppm in aqueous solution,<sup>25</sup> as well as other  $\text{RSNO}$  ( $\text{R} = \text{a variety of groups}$ ) compounds exhibiting  $^{15}\text{N}$  NMR signals at  $\delta = 765$ – $830$  ppm (Scheme 1).<sup>26</sup> Upon the addition of one molar equivalent of  $\text{Na}_2\text{S}$  to the SNAP in DMSO, only one sharp  $^{15}\text{N}$  NMR signal was detected at  $\delta = 710.7$  ppm (Fig. 4b), which we assigned to  $\text{SSNO}^-$ . The addition

of water to this solution caused the signals to shift to lower resonances, and no signals were visible once the percentage of water exceeded 50% (Fig. 4c and d).  $\text{SNO}^-$  was again obtained by adding excess TPH into a freshly prepared  $\text{SSNO}^-$  formulation, and the  $^{15}\text{N}$  signal was detected at  $\delta = 897.9$  ppm. This signal was found to be less stable than that of  $\text{SSNO}^-$  in the presence of water, since no signals were visible once the percentage of water exceeded 30% (Fig. 4e and f). The lack of a signal can be attributed to the long spin-lattice relaxation times of  $^{15}\text{N}$ , which limit the suitability of this technique for the detection of short-lived intermediates. This finding was consistent with our previous findings obtained *via* the  $^{15}\text{N}$  NMR characterization of intermediates  $[\text{Fe}(\text{CN})_5\text{N}(\text{O})\text{S}]^{4-}$  and  $[\text{Fe}(\text{CN})_5\text{N}(\text{O})\text{SS}]^{4-}$  obtained from Gmelin reaction in which  $[\text{Fe}(\text{CN})_5\text{N}(\text{O})\text{S}]^{4-}$  exhibited a  $^{15}\text{N}$  NMR signal at  $\delta = 700$  ppm and  $[\text{Fe}(\text{CN})_5\text{N}(\text{O})\text{SS}]^{4-}$  exhibited  $^{15}\text{N}$  NMR signal at  $\delta = 630$  ppm.<sup>23</sup>

After having established the  $^{17}\text{O}$  NMR signature of  $\text{SNO}^-$  and  $\text{SSNO}^-$ , we turned our attention toward stability (*i.e.*, the half-life) measurements. To this end, we recorded the  $^{17}\text{O}$  NMR spectra and plotted the signal intensity as a function of time for  $\text{SNO}^-$  and  $\text{SSNO}^-$  in different conditions. As reported in previous studies by Feilisch and coworkers, oxygen consumption occurs during the course of this nitrosothiol/sulfide cross-linking reaction.<sup>17</sup>  $\text{SNO}^-$  and  $\text{SSNO}^-$  were therefore prepared under anaerobic conditions to assess their stability, and the preparation methods are described in the caption of Fig. 5. As shown in Fig. 5a,  $\text{SNO}^-$  was rather stable with a half-life of 21 h in the absence of oxygen ( $\text{O}_2$ ) in DMSO, but once water was added to the preparations, the half-life of  $\text{SNO}^-$  had decreased to 87 and 11 min in 30%  $\text{H}_2\text{O}/\text{DMSO}$  and 50%  $\text{H}_2\text{O}/\text{DMSO}$ , respectively (Fig. 5b and c). In comparison, the half-life of  $\text{SNO}^-$  in DMF was found to be 32 min (Fig. 5d), which was much shorter than the value determined in DMSO. This could be due to the presence of trace amounts of  $\text{O}_2$  in DMF. These results indicated that  $\text{SNO}^-$  was unstable in both water and air. Compared with the half-life of  $\text{SNO}^-$ , it was evident that  $\text{SSNO}^-$  was more stable in DMSO under the anaerobic conditions with a half-life of 58 h (Fig. 5e), while in the presence of  $\text{O}_2$  its half-life is reduced to 14 h in DMSO (Fig. 5f). Moreover, the  $\text{SSNO}^-$  species that was prepared by mixing  $\text{GSNO}$  with 2 molar equivalents of  $\text{Na}_2\text{S}$  in phosphate buffer at pH 7.4 exhibited a half-life of only 39 min, and that prepared by mixing  $\text{GSNO} : \text{Na}_2\text{S}$  at a 1 : 1 molar ratio exhibited an even shorter half-life of 18 min. These collectively decomposed quickly under physiological conditions,  $\text{SSNO}^-$  is still much more stable than  $\text{SNO}^-$  and could be used for bioactivity evaluation in cellular assays.<sup>18,19</sup>

It has been suggested that the  $\text{pK}_a$  of  $\text{HSNO}$  exceeds 10.5.<sup>15</sup> Unfortunately, we were unable to experimentally measure the  $\text{pK}_a$  value of  $\text{HSNO}/\text{SNO}^-$  due to its instability in aqueous solution.  $\text{SSNO}^-$  was shown to have greater stability under physiological conditions and its chemical shifts that were determined *via*  $^{17}\text{O}$  and  $^{15}\text{N}$  NMR were less than the chemical shifts of  $\text{SNO}^-$ , suggesting a lower  $\text{pK}_a$  for  $\text{SSNO}^-$ . We have recorded the  $^{17}\text{O}$  NMR spectra of  $\text{SSNO}^-$  at various pH values. Remarkably, the  $^{17}\text{O}$  NMR signal does not show any noticeable change over a pH range from 4.69 to 12.10, neither with regard

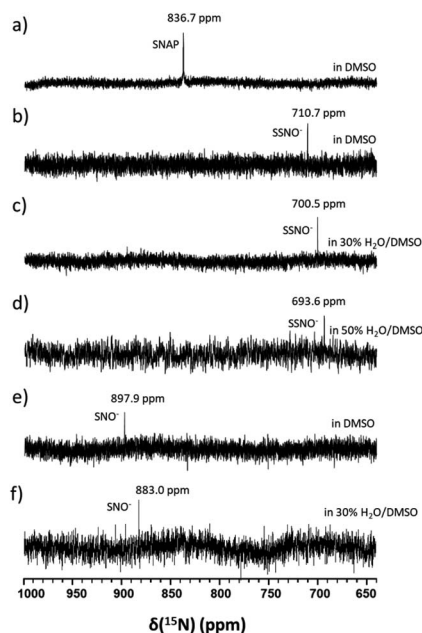
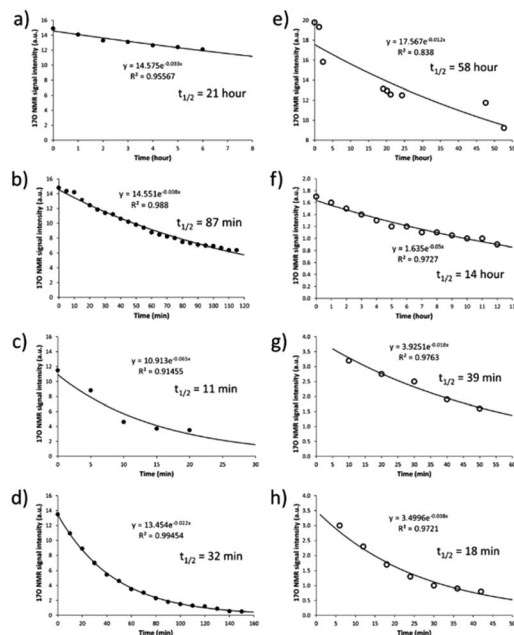


Fig. 4  $^{15}\text{N}$  NMR spectra of (a) 100 mM  $^{15}\text{N}$ -labeled SNAP in DMSO, (b) freshly prepared  $^{15}\text{N}$ -labeled  $\text{SSNO}^-$  that was obtained by mixing 100 mM  $^{15}\text{N}$ -labeled SNAP with 1 molar equivalent of  $\text{Na}_2\text{S}$  in DMSO containing 10%  $\text{D}_2\text{O}$ , (c) water was added to  $\text{SSNO}^-$  (the formulation described in (b)) to obtain 30%  $\text{H}_2\text{O}$  in DMSO, (d) water was added to  $\text{SSNO}^-$  to obtain 50%  $\text{H}_2\text{O}$  in DMSO, (e) freshly prepared  $^{15}\text{N}$ -labeled  $\text{SNO}^-$  that was obtained by adding 3 molar equivalents of TPH to  $\text{SSNO}^-$ , and (f) water was added to  $\text{SNO}^-$  (the formulation described in (e)) to get 30%  $\text{H}_2\text{O}$  in DMSO.





**Fig. 5** Decomposition of  $\text{SNO}^-$  and  $\text{SSNO}^-$  over time as monitored by  $^{17}\text{O}$  NMR spectroscopy (with signals at 1216 and 988 ppm, respectively). In (a),  $\text{SNO}^-$  was prepared under anaerobic conditions (in a glove box) by adding 1 molar equivalent of  $\text{Na}_2\text{S}$  (in  $\text{H}_2\text{O}$ ) to 100 mM  $^{17}\text{O}$ -labeled SNAP in DMSO, and subsequently adding to that solution another DMSO solution containing 3 molar equivalents of TPH. In (b),  $\text{SNO}^-$  was obtained as described in (a) except that  $\text{H}_2\text{O}$  was added to provide a 30%  $\text{H}_2\text{O}$ /DMSO mixture. In (c),  $\text{SNO}^-$  was obtained as described in (a) except that  $\text{H}_2\text{O}$  was added to provide a 50%  $\text{H}_2\text{O}$ /DMSO mixture. In (d),  $\text{SNO}^-$  was obtained under anaerobic conditions by adding 1 molar equivalent of  $\text{Na}_2\text{S}$  (in  $\text{H}_2\text{O}$ ) to 100 mM  $^{17}\text{O}$ -labeled SNAP in DMF, and subsequently adding 6 molar equivalents of TPH in DMF. In (e),  $\text{SSNO}^-$  was obtained under anaerobic conditions by adding 1 molar equivalent of  $\text{Na}_2\text{S}$  (in  $\text{H}_2\text{O}$ ) to 100 mM  $^{17}\text{O}$ -labeled SNAP in DMSO. In (f),  $\text{SSNO}^-$  was obtained by adding 1 molar equivalent of  $\text{Na}_2\text{S}$  (in  $\text{H}_2\text{O}$ ) to 100 mM  $^{17}\text{O}$ -labeled SNAP in DMSO under ambient conditions. In (g),  $\text{SSNO}^-$  was obtained under anaerobic conditions by adding 2 molar equivalents of  $\text{Na}_2\text{S}$  (in  $\text{D}_2\text{O}$ ) to 10 mM  $^{17}\text{O}$ -labeled SNAP in 1 M  $\text{D}_2\text{O}$  phosphate buffer pH 7.4. In (h),  $\text{SSNO}^-$  was obtained by adding 1 molar equivalent of  $\text{Na}_2\text{S}$  (solid) to 50 mM  $^{17}\text{O}$ -labeled GSNO in 1 M  $\text{D}_2\text{O}$  phosphate buffer pH 7.4 under ambient conditions.

to the signal intensity nor its chemical shift (data are shown in Fig. 6). However,  $\text{SSNO}^-$  becomes too unstable below pH 4.69 to be studied by NMR spectroscopy. Nevertheless, the  $^{17}\text{O}$  NMR spectra clearly show that  $\text{SSNO}^-$  has a  $\text{pK}_a$  value of less than 4.69. Thus, the  $\text{SSNO}^-$  anion is the predominate form at physiological pH.

Since  $\text{SNO}^-$  and  $\text{SSNO}^-$  are more stable under anaerobic conditions, we attempted to capture the short lived  $\text{SNO}^-$  species in a freshly prepared cross-linking reaction mixture by adding one molar equivalent of  $\text{Na}_2\text{S}$  to 100 mM  $^{17}\text{O}$ -labelled SNAP in DMSO (under anaerobic conditions) and compared the resultant spectrum to that of an otherwise similar sample that was prepared in air. A very weak signal was observed at 1219 ppm in the  $^{17}\text{O}$  NMR spectrum of this sample that was prepared under anaerobic conditions (Fig. 7a), which we

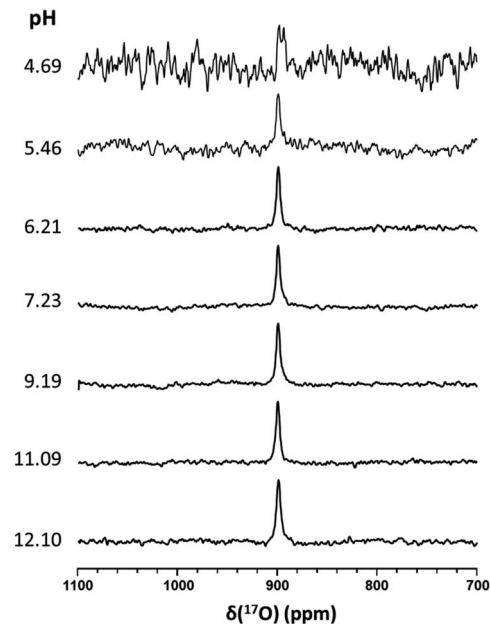


**Fig. 6**  $^{17}\text{O}$  NMR spectra of  $\text{SSNO}^-$  recorded at various pH values.  $\text{SSNO}^-$  was prepared by mixing 10 mM  $^{17}\text{O}$ -labeled GSNO with 1 molar equivalent of  $\text{Na}_2\text{S}$  in 0.5 M phosphate buffer. Different pH values were obtained by adjusting with acidic resin or  $\text{NaOH}$  powder. For each spectrum, a total of ca. 21 664 transients was recorded with a recycle delay of 20 ms (with a total acquisition time of 27 min).

attributed to  $\text{SNO}^-$ . In contrast, this signal at 1219 ppm was not detected in the spectrum of the mixture prepared in air (Fig. 3b).

To further support our findings, a comparison between the  $^{17}\text{O}$  NMR spectra of samples prepared *via* different mixing

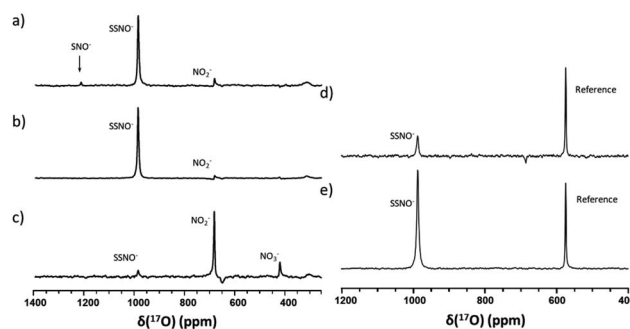


**Fig. 7**  $^{17}\text{O}$  NMR spectra of freshly prepared cross-linking reaction mixtures in DMSO that were obtained *via* different methods under anaerobic conditions. In (a), the mixture was prepared with 200  $\mu\text{L}$  of 200 mM  $^{17}\text{O}$ -SNAP in DMSO with 1 molar equivalent of  $\text{Na}_2\text{S}$  (200  $\mu\text{L}$  of DMSO and 40  $\mu\text{L}$  of 1 M  $\text{Na}_2\text{S}$  in  $\text{D}_2\text{O}$ ). In (b), the mixture was prepared by slowly adding 200  $\mu\text{L}$  of 200 mM  $^{17}\text{O}$ -labeled SNAP solution to 240  $\mu\text{L}$  of  $\text{Na}_2\text{S}$ , *via* 10  $\mu\text{L}$  additions at 2 min intervals. In (c), the mixture was prepared by slowly adding 240  $\mu\text{L}$  of  $\text{Na}_2\text{S}$  solution to 200  $\mu\text{L}$  of 200 mM  $^{17}\text{O}$ -labeled SNAP solution, *via* 10  $\mu\text{L}$  additions at 2 min intervals. In (d) the mixture was prepared with 400  $\mu\text{L}$  100 mM  $^{17}\text{O}$ -labeled SNAP in DMSO with 1 molar equivalent of  $\text{Na}_2\text{S}$  (40  $\mu\text{L}$  1 M  $\text{Na}_2\text{S}$  in  $\text{D}_2\text{O}$ ), with 10%  $^{17}\text{O}$ -labeled nicotinamide used as a reference. In (e), the mixture was prepared with 400  $\mu\text{L}$  of 100 mM  $^{17}\text{O}$ -labeled SNAP in DMSO with 1 molar equivalent of  $\text{Na}_2\text{S}$  (40  $\mu\text{L}$  1 M  $\text{Na}_2\text{S}$  in  $\text{D}_2\text{O}$ ), with 10%  $^{17}\text{O}$ -labeled nicotinamide used as a reference.

methods was undertaken, as seen in Fig. 7b and c. In Fig. 7b, the mixture was prepared by slowly adding 200  $\mu\text{L}$  of 200 mM SNAP to one molar equivalent of  $\text{Na}_2\text{S}$  solution (200  $\mu\text{L}$  DMSO and 40  $\mu\text{L}$  of 1 M  $\text{Na}_2\text{S}$  in  $\text{D}_2\text{O}$ ), *via* 10  $\mu\text{L}$  additions at 2 min intervals. When this method was employed, the resultant  $^{17}\text{O}$  NMR spectrum did not exhibit an  $\text{SNO}^-$  signal, suggesting that in the presence of excess  $\text{HS}^-$ ,  $\text{SNO}^-$  was quickly converted to  $\text{SSNO}^-$ .

This finding was consistent with our observations from the UV-Vis analysis (Fig. 1f), and in accordance with the previous findings by others *via* UV-Vis spectroscopy, where it was found that increasing the molar ratio of  $\text{Na}_2\text{S}$  caused the intermediates to become converted from  $\text{SNO}^-$  to  $\text{SSNO}^-$ .<sup>17</sup> Conversely, when the method was reversed by slowly adding the  $\text{Na}_2\text{S}$  solution to the SNAP solution, neither the  $\text{SNO}^-$  nor the  $\text{SSNO}^-$  signals were detected, and only the signals of decomposed products such as  $\text{NO}_2^-$  and  $\text{NO}_3^-$  anions were detected at  $\delta = 683$  and 425 ppm, respectively (Fig. 7c). This behavior suggested that mixing  $\text{SSNO}^-$  with excess  $\text{HS}^-$  would not lead to the formation of  $\text{SNO}^-$ , but rather to decomposition to  $\text{NO}_2^-$  and  $\text{NO}_3^-$  anions. In addition, we compared the amount of intermediate formed by mixing one molar equivalent of  $\text{Na}_2\text{S}/\text{Na}_2\text{S}_2$  with SNAP, with 10%  $^{17}\text{O}$ -labeled nicotinamide used as an internal reference. As seen in Fig. 7d and e, the signal intensity was much higher if  $\text{Na}_2\text{S}_2$  (which provide  $\text{HSS}^-$  in the reaction) was added instead of  $\text{Na}_2\text{S}$ . This further demonstrated that the  $^{17}\text{O}$  signal at 986.9 ppm represents  $\text{SSNO}^-$ .

After the  $\text{SNO}^-$  and  $\text{SSNO}^-$  were successfully characterized *via* UV-vis and NMR spectroscopy, we further investigated their bioactivity *via* cultured HUVEC. The research undertaken by Koeppenol *et al.* indicated that the formation of  $\text{SSNO}^-$  was thermodynamically unfavorable due to the low concentrations of reactants *in vivo*.<sup>27</sup> In the current study, we prepared the  $\text{SNO}^-$  and  $\text{SSNO}^-$  *via* a chemical reaction *in vitro*, and evaluate their bioactivity accordingly. Cells were grown in the recommended conditions as described in the Experimental Section and respectively treated with SNAP,  $\text{Na}_2\text{S}$ , TPH, and TPH-S alone, as well as with the  $\text{SSNO}^-$ -enriched mixtures of SNAP and  $\text{Na}_2\text{S}$  that were mixed at different molar ratios (SNAP :  $\text{Na}_2\text{S}$  = 1 : 2 and 1 : 5),<sup>17</sup> or with  $\text{SNO}^-$ -enriched mixtures of SNAP,  $\text{Na}_2\text{S}$ , and TPH that were mixed at different molar ratio (SNAP :  $\text{Na}_2\text{S}$  : TPH = 1 : 2:2, 1 : 2:3, 1 : 5:3 and 1 : 5:5). The intracellular concentration of nitric oxide (NO) in live cells after these treatments was measured with a NO indicator, 3-amino,4-aminomethyl-2',7'-difluorescein, diacetate (DAF-FM DA). HUVEC were initially incubated with this NO probe which can freely cross cell membranes. Once inside the cells, the probe can react with NO and generate a strong fluorescence signal, which can then be analyzed *via* flow cytometry.<sup>28</sup> After the treatments were applied to cells, higher levels of intracellular NO would be revealed by increased fluorescence intensities, as shown in Fig. 8, NC groups contained only the NO probe, without receiving any of the treatments listed above, and were employed to measure the endogenous NO that initially resided in the cells. Respective treatments with  $\text{Na}_2\text{S}$ , TPH, and TPH-S alone showed little effect on the NO concentration. Conversely, cells treated with  $\text{SSNO}^-$ -enriched mixtures of SNAP

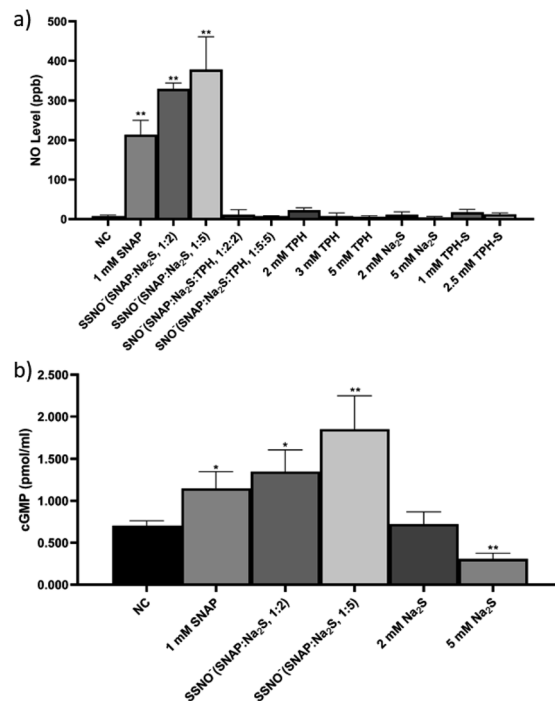


Fig. 8 (a) The cellular NO levels as determined in HUVEC after had received various treatments, including SNAP,  $\text{Na}_2\text{S}$ , TPH,  $\text{SSNO}^-$ -enriched mixture, and  $\text{SNO}^-$ -enriched mixture. (b) The cGMP levels as observed in HUVEC after these cells had received various treatments. \* $p < 0.05$ , \*\* $p < 0.01$ , compared to NC. HUVEC: human umbilical vein endothelial cells, cGMP: cyclic guanosine monophosphate.

and  $\text{Na}_2\text{S}$  (at both 1 : 2 and 1 : 5 molar ratios) showed a substantial elevation of the NO concentrations, suggesting that  $\text{SSNO}^-$  increased the intracellular NO levels in HUVEC. In contrast, no significant increase of NO levels was observed in cells that were treated with  $\text{SNO}^-$ -enriched mixtures, suggesting that  $\text{SNO}^-$  does not exhibit NO releasing behavior in cell cultures. This could be due to the instability of  $\text{SNO}$  under physiological conditions and this finding was consistent with our  $^{17}\text{O}$  NMR measurements of the half-life values of  $\text{SNO}^-$  and  $\text{SSNO}^-$  (Fig. 5).

Although the DAF-FM DA NO detection assays suggested an elevation of intracellular NO concentration in  $\text{SSNO}^-$  treated cell cultures, the method also encountered limitations in the presence of oxidants/antioxidants, which interfere with the results by potentially modifying the steady-state concentration of the  $\text{NO}^\bullet$  radical.<sup>29</sup> Therefore, the release of NO by  $\text{SSNO}^-$  in cells was further demonstrated by determining the changes in cGMP levels, as cGMP is a downstream marker of NO signaling and is involved in the regulation of vascular tone.<sup>30</sup> As shown in Fig. 8e, the cGMP concentration did not change significantly with 2 mM  $\text{Na}_2\text{S}$ , but treatment with 5 mM  $\text{Na}_2\text{S}$  decreased the cGMP concentration in cells. Meanwhile, treatment with  $\text{SSNO}^-$ -enriched mixtures increased the cGMP levels in the cells regardless of the negative effect of excess  $\text{Na}_2\text{S}$ , indicating that  $\text{SSNO}^-$  strongly increased the cGMP level through a NO-dependent signaling pathway. This effect was also proven in previous studies, where elevated cGMP levels were detected





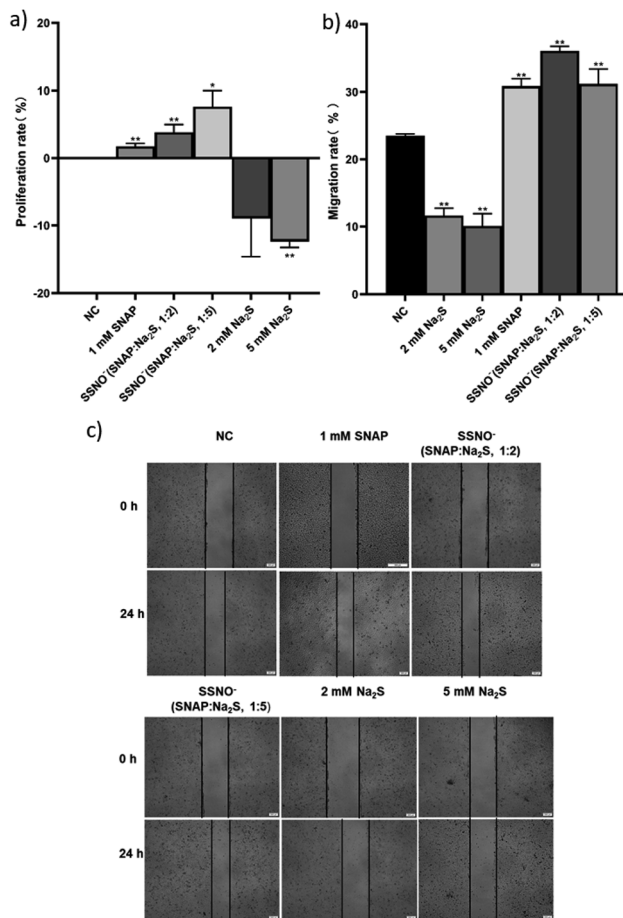


Fig. 9 The proliferation and migration of HUVEC was assessed with the treatment of SNAP, Na<sub>2</sub>S, and SSNO<sup>-</sup>-enriched mixtures. (a) Cell proliferation rate determined after the above treatments, (b) migration rate comparison among the treatment groups, and (c) photographs taken under 100× magnification. \**p* < 0.05, \*\**p* < 0.01, compared to the NC group.

after RFL-6 cells had been treated with SSNO<sup>-</sup>-enriched mixtures.<sup>17,22</sup> These results showed the potential bioactivity of SSNO<sup>-</sup> in NO-cGMP-dependent vasodilation.

Ondrias and coworkers have previously suggested that the products obtained *via* cross-linking reactions between RSNO and sulfide moieties could be a potent vasorelaxants.<sup>18</sup> To this end, we evaluated the effect of SSNO<sup>-</sup> in promoting angiogenesis, as angiogenesis and vasodilation accompany one another *in vivo* and NO can mediate angiogenesis.<sup>31,32</sup> As seen in Fig. 9a, SSNO<sup>-</sup>-enriched mixtures of SNAP and Na<sub>2</sub>S promoted HUVEC proliferation regardless of the negative effects that are presented by excess Na<sub>2</sub>S in the cell culture. Scratched wound healing assays were utilized to assess the migration capabilities of cells that had been treated with SSNO<sup>-</sup>-enriched mixtures. The scratched area was measured *via* Image J software. In comparison to the initial wound area, cells that had been treated with SNAP or with SSNO<sup>-</sup>-enriched mixtures of SNAP and Na<sub>2</sub>S (1 : 2 and 1 : 5 molar ratio) showed a significant reduction in the wound area after 24 h incubation, while treatment with Na<sub>2</sub>S (2 and 5 mM) alone resulted in only a slight

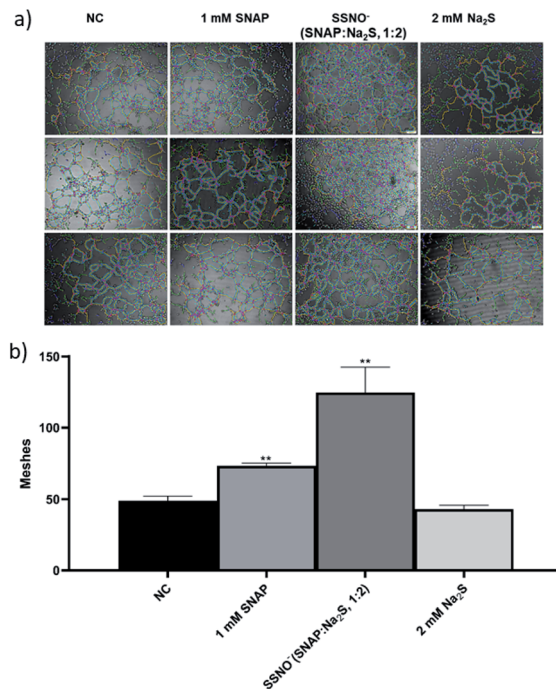


Fig. 10 The proliferation of HUVEC was assessed with the treatment of SNAP, Na<sub>2</sub>S, and a SSNO<sup>-</sup>-enriched mixture using the endothelial cell tube formation assay. (a) Photographs taken under 400× magnification, and (b) comparison of the numbers of meshes among the treatment groups, \**p* < 0.05, \*\**p* < 0.01, compared to NC.

reduction in the wound area (Fig. 9c). The slower wound area closure rate observed in cells treated with 2 and 5 mM Na<sub>2</sub>S could be due to the cytotoxicity of Na<sub>2</sub>S during prolonged incubation, as it was also observed that treatment with Na<sub>2</sub>S inhibited cell proliferation (Fig. 9a). The migration rate was calculated by the equation: migration rate = ( $W_0 - W_t$ )/ $W_0$ , where  $W_0$  is the initial wound area, and  $W_t$  is the wound area after 24 h of incubation. As seen in Fig. 9b, the migration rate of HUVEC was significantly reduced in the Na<sub>2</sub>S treatment groups, but increased in the groups treated with SNAP and the SSNO<sup>-</sup>-enriched mixtures in comparison to the NC group, thus demonstrating the cell migration promoting properties of SSNO<sup>-</sup>.

Moreover, tube forming assays were also employed to evaluate the angiogenesis promoting effect of SSNO<sup>-</sup>-enriched mixtures. HUVEC are the commonly used cell line to study the angiogenesis *in vitro*.<sup>33</sup> The photographs were taken under 400× magnification (Fig. 10a) and the numbers of meshes were counted in order to evaluate the ability of cells to form tubes in 3D culturing conditions (Fig. 10b). Both SNAP and the SSNO<sup>-</sup>-enriched mixture were found to significantly increase the number of meshes in cells, which was not achieved with Na<sub>2</sub>S.

## Conclusions

In summary, we have characterized the intermediates from the cross-linking reaction between H<sub>2</sub>S and NO *via* UV-Vis spectroscopy and provided for the first time the <sup>15</sup>N and <sup>17</sup>O NMR



data for previously elusive  $\text{SNO}^-$  and  $\text{SSNO}^-$  intermediates. Moreover, the  $^{17}\text{O}$  NMR data indicated that  $\text{SSNO}^-$  has a  $\text{pK}_a$  value of less than 4.7. Thus, the  $\text{SSNO}^-$  anion is the predominant species at physiological pH. We have also discovered that the  $\text{SNO}^-$  was rapidly converted to  $\text{SSNO}^-$  and was less stable than  $\text{SSNO}^-$ . *In vitro*  $\text{SNO}^-$  and  $\text{SSNO}^-$  bioactivity analysis suggested that  $\text{SSNO}^-$  acts as a NO-releasing intermediate in cells, increases cellular cGMP levels, and facilitates angiogenesis *in vitro* through a NO-cGMP dependent signaling pathway. We hope that our research will contribute toward a better understanding of the  $\text{H}_2\text{S}$  and NO cross-linking reaction as well as the chemical and biological characteristics of the reaction intermediates. In addition, we hope to encourage others to consider  $^{17}\text{O}$  NMR spectroscopy as a promising new method to probe short-lived reaction intermediates.

## Experimental

### Materials and methods

Chemicals were obtained from Sigma-Aldrich unless otherwise stated. These included sodium hydroxide (NaOH), sulfuric acid ( $\text{H}_2\text{SO}_4$ ), sodium sulfide ( $\text{Na}_2\text{S} \cdot 9\text{H}_2\text{O}$ ), sodium nitrite ( $\text{NaNO}_2$ ),  $^{15}\text{N}$ -labeled sodium nitrite ( $\text{Na}^{15}\text{NO}_2$ , 98%  $^{15}\text{N}$ ),  $^{17}\text{O}$ -labeled water ( $\text{H}_2^{17}\text{O}$ , 41.1%  $^{17}\text{O}$ , purchased from CortecNet), L-glutathione (GSH), N-acetyl-D-penicillamine (NAP), monosodium phosphate ( $\text{NaH}_2\text{PO}_4$ ), disodium phosphate ( $\text{Na}_2\text{HPO}_4$ ), triphenylphosphine, dimethyl sulfoxide (DMSO), dimethylformamide (DMF), deuterium oxide ( $\text{D}_2\text{O}$ , CIL), acetone- $d_6$  (CIL), Matrigel (Corning), 3-(4,5-di-methylthiazol-2-yl)-2,5-diphenyl tetrazolium bromide (MTT), and ion-exchange resin (Amberlite IR-120, strongly acidic form). HUVEC was obtained from the Cell Bank of the Committee on Type Culture Collection of Chinese Academy of Sciences (Shanghai, China). Complete cell growth medium RPMI 1640 (Thermo Fisher Scientific, Shanghai, China) containing 10% fetal bovine serum (FBS, Thermo Fisher Scientific) and 1% penicillin/streptomycin (Thermo Fisher Scientific) were used to grow cells. The levels of NO and cGMP within the cells was determined with the use of DAF-FM DA (NO detection kit, Beyotime Biotechnology) and cGMP ELISA detection kit (GenScript).

### Synthesis of isotope-labelled compounds

$^{15}\text{N}$ -Labelled SNAP was prepared according to the literature method.<sup>34</sup> NAP (191.2 mg) was mixed with 1.1 molar equivalents of  $\text{Na}^{15}\text{NO}_2$  in 0.58 mL of 0.55 M HCl. The reaction mixture was kept on ice for 40 min prior to the addition of 10  $\mu\text{L}$  of concentrated  $\text{H}_2\text{SO}_4$ . The product was collected by filtration, washed with ice-cold water ( $5 \times 2\text{ mL}$ ), and subsequently dried under vacuum to give a green powder (120 mg, 63% yield). The  $^{15}\text{N}$  enrichment of the product was 98%.  $^{15}\text{N}$  NMR (40.6 MHz, acetone- $d_6$ ):  $\delta = 835\text{ ppm}$  (ref. to liquid  $\text{NH}_3$ ).  $^{15}\text{N}$  NMR (50.6 MHz, DMF):  $\delta = 836.7\text{ ppm}$ .

$^{17}\text{O}$ - $\text{NaNO}_2$  was (0.8 g, 11.6 mmol) was dissolved in 40%  $^{17}\text{O}$ -labelled  $\text{H}_2\text{O}$  (M wt. 19–20, 1 g, 50 mmol) in acidic condition. The mixture was stirred slowly for 20 min until a solution was obtained. This solution was heated overnight at 75  $^\circ\text{C}$ .  $^{17}\text{O}$ -

$\text{NaNO}_2$  signal was recorded at 661.15 ppm. The sample was then lyophilized overnight.

$^{17}\text{O}$ -SNAP was prepared in 0.5 mL of 0.55 M HCl (in  $\text{H}_2^{17}\text{O}$ , 41.1%  $^{17}\text{O}$ ) by mixing NAP (231.1 mg) with 1.1 molar equivalents of  $\text{Na}^{17}\text{O}_2$ . The work-up procedures were similar to that used in the preparation of the  $^{15}\text{N}$ -labeled SNAP. The  $^{17}\text{O}$  enrichment of the product was 30%.  $^{17}\text{O}$  NMR (54.3 MHz, acetone- $d_6$ ):  $\delta = 1314\text{ ppm}$  (ref. to water).  $^{17}\text{O}$  NMR (67.7 MHz, DMF):  $\delta = 1312\text{ ppm}$ .  $^{17}\text{O}$  NMR (67.7 MHz, PB buffer pH 7.41):  $\delta = 1296\text{ ppm}$ .  $^{17}\text{O}$  NMR (67.7 MHz, DMSO- $d_6$ ):  $\delta = 1307\text{ ppm}$ . FWHH = 2053 Hz (line broadening = 20).

$^{15}\text{N}$ -GSNO was prepared according to the literature method.<sup>35</sup> GSH (150 mg) was mixed with 1.1 molar equivalents of  $\text{Na}^{15}\text{NO}_2$  in 1 mL of 0.48 M HCl. The reaction mixture was kept on ice for 40 min prior to the addition of 3 mL of ice-cold acetone, and subsequently stirred for 10 min. The product was collected by centrifugation at 3000 rpm for 2 min. The supernatant was discarded. The residue was resuspended in acetone. This process was repeated 3 times. The residue was dried under a flow of Ar gas and left under vacuum to give a pink powder (69 mg, 46% yield).  $^{15}\text{N}$  NMR (40.6 MHz,  $\text{D}_2\text{O}$ ):  $\delta = 768\text{ ppm}$  (ref. to liquid  $\text{NH}_3$ ).

$^{17}\text{O}$ -GSNO was prepared in 0.58 mL of 0.55 M HCl (in  $\text{H}_2^{17}\text{O}$ , 41.1%  $^{17}\text{O}$ ) by mixing GSH (150 mg) with 1.1 molar equivalents of  $\text{Na}^{17}\text{O}_2$ . The work-up procedures were the same as that used to prepare the  $^{15}\text{N}$ -labeled GSNO. The  $^{17}\text{O}$  enrichment of the product was 30%.  $^{17}\text{O}$  NMR (54.3 MHz,  $\text{D}_2\text{O}$ ):  $\delta = 1211\text{ ppm}$  (ref. to water).

**Preparation of  $\text{SSNO}^-$  and  $\text{SNO}^-$ -enriched mixtures.**  $\text{SSNO}^-$ -enriched mixtures were prepared by mixing SNAP with  $\text{Na}_2\text{S}$  at various molar ratios in different solvents under aerobic or anaerobic conditions as indicated in the Fig legends.  $\text{SNO}^-$ -enriched mixtures were prepared *via* the addition of various molar equivalents of TPH into the  $\text{SSNO}^-$ -enriched mixtures under different conditions as indicated in the Fig legends. For the cell cultures, a high concentration of  $\text{Na}_2\text{S}$  stock solution (0.5 M) was freshly prepared with 0.5 M phosphate buffer at pH 7.4, and PBS was then used to dilute this solution to lower concentrations. These solutions were then mixed with SNAP at various ratios as indicated in the figures.

**Measurement of cellular NO level.** Cellular NO levels were determined with the DAF-FM DA NO detection kit. Briefly, HUVEC were seeded in 6-well plates at a density of  $3 \times 10^5$  cells per well and grown to reach 100% confluence. The medium was gently aspirated with a pipette before 1 mL of the probe (1 : 1000 dilution of the original solution) was added to each well. Plates were placed into a plate shaker and incubated for 20 min. The probe was then aspirated and the wells were washed twice with PBS (pH 7.4) to remove the remaining probe. HUVEC were then treated with SNAP,  $\text{Na}_2\text{S}$ , TPH, TPH-S,  $\text{SNO}^-$  and  $\text{SSNO}^-$ -enriched mixtures in serum free medium accordingly for 20 min. The medium was then aspirated from the wells and washed once with PBS gently. Cells were trypsinized for 3 min and then neutralized by adding complete growth medium. Cell pellets were collected by centrifugation, washed with PBS, and re-suspended in 500  $\mu\text{L}$  of PBS in flow cytometry tubes, covered with aluminum foil, and finally analyzed *via* flow cytometry.





**Measurement of cellular cGMP levels.** Cellular cGMP levels were determined *via* a cGMP ELISA Detection kit according to the manufacturer's instructions. Briefly, HUVEC were seeded into 6-well plates at a density of  $3 \times 10^5$  cells per well and grown to reach 100% confluence. The growth medium was then replaced with SNAP,  $\text{Na}_2\text{S}$ , and  $\text{SSNO}^-$ -enriched mixtures in serum-free medium. After 20 min of incubation, the medium was aspirated and 100  $\mu\text{L}$  of RIPA lysis buffer was added and each sample was incubated for 20 min. The cells were scraped from the wells using a cell scraper, centrifuged at 2000 rpm for 10 min, and the supernatants were then collected. To prepare an ELISA plate for cGMP detection, 100  $\mu\text{L}$  of Anti-cGMP pAb was added to each well of a blank ELISA plate. Plates were sealed and incubated at 25  $^\circ\text{C}$  for 45 min to achieve an optimal linking. After incubation, wells were washed 4 times with 260  $\mu\text{L}$  of washing solution. Subsequently, the plate was inverted on absorbent paper to remove residual liquid from the wells. Assay buffer A (100  $\mu\text{L}$ ) was added to the non-specific binding (NSB) wells; 100  $\mu\text{L}$  of standard cGMP solutions at concentrations of 0, 0.3, 0.8, 2.5, 7.4, 22.2, 66.7  $\text{pmol mL}^{-1}$  were added to the calibration wells, and cell supernatants were added to the remaining wells. After this step, 50  $\mu\text{L}$  of assay buffer B was added to the NSB well, and 50  $\mu\text{L}$  of cGMP-HRP was added to the remaining wells. After 1 h of incubation at 4  $^\circ\text{C}$ , plates were washed 4 times with 260  $\mu\text{L}$  of washing solution and the residual liquid in the wells was removed. TMB (100  $\mu\text{L}$ ) was then added to all of the wells and further incubated at 25  $^\circ\text{C}$  in the dark for 20 min. Finally, 50  $\mu\text{L}$  of stop solution was added to all of the wells to stop the reaction. The absorbance of each well was measured at OD 450 nm *via* an enzyme-linked immunosorbent detector.

**Measurement of cell proliferation.** The cell proliferation effect was evaluated with MTT assays. HUVEC were seeded in 96-well plates at a density of 8000 cells per well and incubated for 24 h to reach 70% confluence. The complete growth medium was replaced with serum-free medium containing SNAP,  $\text{Na}_2\text{S}$ , and  $\text{SSNO}^-$  in the corresponding wells, and further incubated for 24 h. MTT (10  $\mu\text{L}$ , 5  $\text{mg mL}^{-1}$ ) was then added to each well and the reaction was allowed to proceed for another 4 h. Finally, 150  $\mu\text{L}$  of DMSO was added to each well and the plate was agitated on a plate shaker for 3 min. The cell viability was determined using a microplate reader at wavelengths of 490 and 560 nm.

**Measurement cell migration.** Cell migration was studied using scratch assays. HUVEC were seeded in 6-well plates at a density of  $3 \times 10^5$  cells per well and grew to reach 100% confluence. The scratches were made through the monolayer in the middle of each plate using 200  $\mu\text{L}$  pipette tips. Wells were washed 3 times with PBS to remove floating cells. Cells were then treated with SNAP,  $\text{Na}_2\text{S}$ , and  $\text{SSNO}^-$ -enriched mixtures in serum free medium. After 24 h of incubation, images were obtained with an Olympus BX53 microscope.

**Measurement angiogenesis.** *In vitro* angiogenesis was examined using Matrigel-based (a liquid laminin/collagen gel) endothelial cell tube formation assay. Briefly, 20  $\mu\text{L}$  per well of Matrigel were added into 96-well plates. While waiting for

Matrigel to solidify, cells were trypsinized and resuspended using fresh growth medium. After the Matrigel had solidified, HUVEC were seeded in 96-well plates containing Matrigel at a density of  $3 \times 10^4$  cells per well. Subsequently, SNAP,  $\text{Na}_2\text{S}$ , and  $\text{SSNO}^-$ -enriched mixture were added to the corresponding wells and incubated for 4 h. Cells were observed using a microscope (Olympus BX53).

## Conflicts of interest

There are no conflicts to declare.

## Acknowledgements

Y. G. thanks the National Natural Science Foundation of China [grant number 31700713]; the Department of Science and Technology of Jilin Province [grant number 20200801066GH] for financial support.

## Notes and references

- 1 B. Olas, *Clin. Chim. Acta*, 2015, **439**, 212–218.
- 2 S. Cacanyiova, A. Berenyiova and F. Kristek, *Physiological Research*, 2016, **65**, S273–S289.
- 3 D. J. Polhemus and D. J. Lefer, *Circ. Res.*, 2014, **114**, 730–737.
- 4 H. Kimura, *Nitric Oxide*, 2014, **41**, 4–10.
- 5 M. Y. Ali, C. Y. Ping, Y. Y. Mok, L. Ling, M. Whiteman, M. Bhatia and P. K. Moore, *Br. J. Pharmacol.*, 2006, **149**, 625–634.
- 6 G. Yang, L. Wu, B. Jiang, W. Yang, J. Qi, K. Cao, Q. Meng, A. K. Mustafa, W. Mu, S. Zhang, S. H. Snyder and R. Wang, *Science*, 2008, **322**, 587–590.
- 7 S. Koike, Y. Ogasawara, N. Shibuya, H. Kimura and K. Ishii, *FEBS Lett.*, 2013, **587**, 3548–3555.
- 8 Y. Kimura, Y. Mikami, K. Osumi, M. Tsugane, J. Oka and H. Kimura, *FASEB J.*, 2013, **27**, 2451–2457.
- 9 M. Eberhardt, M. Dux, B. Namer, J. Miljkovic, N. Cordasic, C. Will, T. I. Kichko, J. de la Roche, M. Fischer, S. A. Suarez, D. Bikiel, K. Dorsch, A. Leffler, A. Babes, A. Lampert, J. K. Lennerz, J. Jacobi, M. A. Marti, F. Doctorovich, E. D. Hogestatt, P. M. Zygmunt, I. Ivanovic-Burmazovic, K. Messlinger, P. Reeh and M. R. Filipovic, *Nat. Commun.*, 2014, **5**, 4381.
- 10 K. Ondrias, A. Stasko, S. Cacanyiova, Z. Sulova, O. Krizanov, F. Kristek, L. Malekova, V. Knezl and A. Breier, *Pflügers Arch.*, 2008, **457**, 271–279.
- 11 M. M. Cortese-Krott, B. O. Fernandez, M. Kelm, A. R. Butler and M. Feelisch, *Nitric Oxide*, 2015, **46**, 14–24.
- 12 M. M. Cortese-Krott, A. R. Butler, J. D. Woollins and M. Feelisch, *Dalton Trans.*, 2016, **45**, 5908–5919.
- 13 R. Wedmann, I. Ivanovic-Burmazovic and M. R. Filipovic, *Interface Focus*, 2017, **7**, 20160139.
- 14 I. Ivanovic-Burmazovic and M. R. Filipovic, *Inorg. Chem.*, 2019, **58**, 4039–4051.
- 15 M. R. Filipovic, J. Miljkovic, T. Nauser, M. Royzen, K. Klos, T. Shubina, W. H. Koppenol, S. J. Lippard and I. Ivanovic-Burmazovic, *J. Am. Chem. Soc.*, 2012, **134**, 12016–12027.



- 16 C. L. Bianco and J. M. Fukuto, *Proc. Natl. Acad. Sci. U. S. A.*, 2015, **112**, 10573–10574.
- 17 M. M. Cortese-Krott, B. O. Fernandez, J. L. Santos, E. Mergia, M. Grman, P. Nagy, M. Kelm, A. Butler and M. Feelisch, *Redox Biol.*, 2014, **2**, 234–244.
- 18 A. Berenyiova, M. Grman, A. Mijuskovic, A. Stasko, A. Misak, P. Nagy, E. Ondriasova, S. Cacanyiova, V. Brezova, M. Feelisch and K. Ondrias, *Nitric Oxide*, 2015, **46**, 123–130.
- 19 M. M. Cortese-Krott, D. Pullmann and M. Feelisch, *Pharmacol. Res.*, 2016, **113**, 490–499.
- 20 R. Wedmann, A. Zahl, T. E. Shubina, M. Durr, F. W. Heinemann, B. E. Bugenhagen, P. Burger, I. Ivanovic-Burmazovic and M. R. Filipovic, *Inorg. Chem.*, 2015, **54**, 9367–9380.
- 21 J. P. Marcolongo, U. N. Morzan, A. Zeida, D. A. Scherlis and J. A. Olabe, *Phys. Chem. Chem. Phys.*, 2016, **18**, 30047–30052.
- 22 M. M. Cortese-Krott, G. G. Kuhnle, A. Dyson, B. O. Fernandez, M. Grman, J. F. DuMond, M. P. Barrow, G. McLeod, H. Nakagawa, K. Ondrias, P. Nagy, S. B. King, J. E. Saavedra, L. K. Keefer, M. Singer, M. Kelm, A. R. Butler and M. Feelisch, *Proc. Natl. Acad. Sci. U. S. A.*, 2015, **112**, E4651–E4660.
- 23 Y. Gao, A. Toubaei, X. Kong and G. Wu, *Chemistry*, 2015, **21**, 17172–17177.
- 24 D. Tsikas and A. Bohmer, *Nitric Oxide*, 2017, **65**, 22–36.
- 25 Y. Gao, B. Mossing and G. Wu, *Dalton Trans.*, 2015, **44**, 20338–20343.
- 26 W. Kun, H. Yongchun, Z. Wei, M. B. Ksebati, X. Ming, J.-P. Cheng and P. G. Wang, *Bioorg. Med. Chem. Lett.*, 1999, **9**, 2897–2902.
- 27 W. H. Koppenol and P. L. Bounds, *Arch. Biochem. Biophys.*, 2017, **617**, 3–8.
- 28 C. J. Ku, W. Karunarathne, S. Kenyon, P. Root and D. Spence, *Anal. Chem.*, 2007, **79**, 2421–2426.
- 29 M. M. Cortese-Krott, A. Rodriguez-Mateos, G. G. Kuhnle, G. Brown, M. Feelisch and M. Kelm, *Free Radicals Biol. Med.*, 2012, **53**, 2146–2158.
- 30 F. Z. Monica, K. Bian and F. Murad, *Adv. Pharmacol.*, 2016, **77**, 1–27.
- 31 M. Ziche and L. Morbidelli, *Journal of Neuro-Oncology*, 2000, **50**, 139–148.
- 32 A. Papapetropoulos, G. Garcia-Cardena, J. A. Madri and W. C. Sessa, *J. Clin. Invest.*, 1997, **100**, 3131–3139.
- 33 J. M. Quesada-Gomez, R. Santiago-Mora, C. Navarro-Valverde, G. Dorado and A. Casado-Diaz, *J. Steroid Biochem. Mol. Biol.*, 2015, **148**, 214–218.
- 34 D. Tsikas, D. O. Stichtenoth, R. H. Boger, S. M. Bode-Boger and J. C. Frolich, *J. Labelled Compd. Radiopharm.*, 1994, **34**, 1055–1062.
- 35 T. W. Hart, M. B. Vine and N. R. Walden, *Tetrahedron Lett.*, 1985, **26**, 3879–3882.

